6-8-2021

Energy Harvesting Device for Powering Onboard Condition Monitoring Modules in Rail Service

Martin Amaro Jr.
The University of Texas Rio Grande Valley

Constantine Tarawneh
The University of Texas Rio Grande Valley, constantine.tarawneh@utrgv.edu

Heinrich D. Foltz
The University of Texas Rio Grande Valley, heinrich.foltz@utrgv.edu

Roberto A. Garcia
The University of Texas Rio Grande Valley

Proceedings of the 2021 Joint Rail Conference
JRC2021
April 20-21, 2021, Virtual, Online

JRC2021-58326

ENERGY HARVESTING DEVICE FOR POWERING ONBOARD CONDITION MONITORING MODULES IN RAIL SERVICE

Martin Amaro Jr.
Department of Mechanical Engineering
The University of Texas Rio Grande Valley
University Transportation Center for Railway Safety
Edinburg, TX, 78539, USA
martin.amaro01@utrgv.edu

Constantine Tarawneh, Ph.D.
Department of Mechanical Engineering
The University of Texas Rio Grande Valley
University Transportation Center for Railway Safety
Edinburg, TX, 78539, USA
constantine.tarawneh@utrgv.edu

Heinrich Foltz, Ph.D.
Department of Electrical and Computer Engineering
The University of Texas Rio Grande Valley
University Transportation Center for Railway Safety
Edinburg TX, 78539, USA
heinrich.foltz@utrgv.edu

Roberto A. Garcia
Department of Mechanical Engineering
University Transportation Center for Railway Safety
The University of Texas Rio Grande Valley
Edinburg, TX, 78539, USA
roberto.a.garcia01@utrgv.edu

ABSTRACT

Rail transportation plays an important role in today's economy by delivering a large quantity of goods and passengers to various locations throughout North America in an economic and efficient manner. Bearing failure is one of the leading causes of derailments that result in significant capital loss and in extreme cases tragic human loss. The two widely used bearing health monitoring systems are the Trackside Acoustic Detection System (TADS^{TM}) and the wayside Hot-Box Detector (HBD). These systems are reactive in nature and only give alerts when the bearings are nearing failure. To supplant that, a prototype wireless onboard condition monitoring system was developed by researchers at the University Transportation Center for Railway Safety (UTCRS). This onboard wireless system can detect bearing defects at their early stages of initiation so that proactive maintenance actions can be taken by the railroads and railcar owners. Due to the wireless nature of this system, a constant power supply is needed to ensure its continued operation.

Currently, the prototype wireless system utilizes low-power circuitry that is powered by a rechargeable AA battery that can provide up to two years of operation depending on usage. Implementation of a suitable energy harvesting device can significantly increase the longevity of the batteries used in the wireless module, and in ideal operating conditions, generate consistent energy rendering the battery as a temporary energy storage device. *The proposed energy harvesting device consists of thermoelectric generators, aluminum heat sinks, a switching boost convertor, and a battery management chip. This device was tested on a dynamic bearing test rig to assess the performance of the thermoelectric generators. To best simulate field operation conditions, the thermoelectric generators were placed on opposite sides of the bearing adapter; one exposed to direct forced convection while the other side is shielded by the adapter and experiences minimal convection. Thermoelectric generators were found to be an effective solution due to their ability to convert a temperature gradient into a usable voltage sufficient to charge the battery. The buck booster converter increases the voltage from the thermoelectric generators to 5-volts so that the battery management chip can regulate the voltage and efficiently charge the battery. This paper summarizes the performance of the thermoelectric modules under different operating conditions. The main goal of this project is to devise an energy harvesting device that allows the wireless module to be self-powered utilizing the heat generated from the bearing and the charge held by the battery as a hybrid power source.*

Keywords: Energy harvesting, thermoelectric generators, health monitoring modules, rolling-stock condition monitoring.

NOMENCLATURE

P_{opt}	Optimal theoretical power
R_{opt}	Optimal Resistance
V_{oc}	Open circuit voltage
I_{sc}	Short circuit current
k	thermal conductivity of material

INTRODUCTION

Bearing health monitoring is important in the railway industry as it can prevent delays, high maintenance costs, and derailments. Even so, the two most popular bearing health monitoring systems, the Trackside Acoustic Detection System (TADS^{TM}) and the wayside Hot-Box Detector (HBD), are limited in terms of quantity and efficacy. These wayside devices can only be found along heavy traffic sections of railroad and are few and far between. Moreover, these devices are reactive in nature, i.e., they mostly identify bearings that are nearing catastrophic failure, which requires immediate train stoppage resulting in costly delays. With that in mind, the University Transportation Center for Railway Safety (UTCRS) has developed a wireless onboard condition monitoring module that can continuously gauge the health of the bearing and identify defective bearings at the early stages of defect initiation allowing for proactive maintenance.

To ensure the continuous functionality of the wireless onboard health monitoring module, a consistent and manageable power source that does not depend solely on battery life is needed. One viable option is the use of energy harvesting devices. Energy harvesting is based on the principle that there are power losses in all electrical and mechanical systems that can be repurposed or harvested to power other devices. Examples of this are using ambient energy from radio transmissions or the vibrations in a traveling vehicle as a power source by means of power-transforming transducers. To maximize the efficiency of collecting the ambient energy, it is important to use a harvesting method that functions independently of changing weather conditions. In our current application, the heat produced by a railcar bearing is sufficient to serve as a voltage source when using a thermoelectric module to capture and transform the thermal energy, at any reasonable ambient temperature. This practice allows for power to “trickle” into an intermediary power storage device such as a rechargeable battery. The latter is necessary because the thermoelectric module will not always generate enough power to operate the intended device, but by using a rechargeable battery to store the dynamic power input, a consistent voltage can be delivered. This is similar in practice to lawn lights that charge a battery with a solar panel during the day to serve as a light source at night. However, instead of an LED light, a similar strategy is employed to power a wireless onboard bearing condition monitoring module. Naturally, because this power management system requires a heat source, it will only function once the railcar is in motion and operating under load. Weight and motion place a strain on the bearing, with resisting frictional forces causing it to generate heat. This is in line with the goals of the power delivery system, as bearing health warnings are most relevant when the railcar is in motion.

This paper explores the science and function of thermoelectric generators along with their suitability and performance as a dependable power source for this intended application. To that end, the energy harvesting system, composed of a thermoelectric generator and an aluminum heatsink, is placed on a dynamic bearing test rig that simulates the load and rotational velocity that a bearing experiences in typical rail service. A buck booster converter will later be used to step up the voltage so that the battery will charge consistently, as the power generated is in the range of 50 mW at optimal conditions.

Thermoelectric Generators

Thermoelectric generators (TEGs) can convert energy dissipated as heat into electricity. This is accomplished using the Seebeck effect, which is the phenomenon where a voltage is produced by having a temperature gradient between two surfaces that are connected by semiconductors. Both surfaces are made of a ceramic substrate and have a “hot” side and a “cold” side. Since there is a temperature gradient between both ceramic surfaces the heat is transferred from the hot side through the semiconductors and into the cold side.

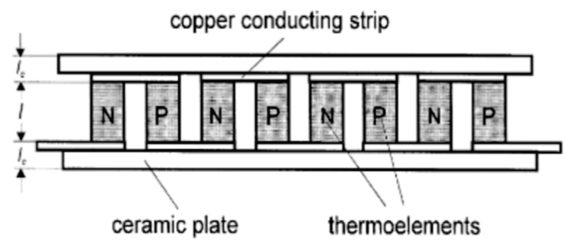

Figure 1: Thermoelectric Generator Schematic [1]

The TEG devices use two different types of semiconductors that include P-type and N-type. Although both semiconductors are made of the same material, they have different electron density which causes the charge from the energy transfer to go through the respective semiconductor. Because the semiconductors are connected in series, they build up charge on their terminals, which creates the voltage potential across the entire module.

One of the main advantages of thermoelectric generators are their solid-state build, meaning that there are no moving parts that make them susceptible to failure, thus, rendering them maintenance free [1-2]. This is advantageous in our application since railcars operate for millions of miles during their lifespan and the generators will not be susceptible to the random vibrations that railcars experience in rail service. Additionally, unlike solar or wind harvesting, which depend on fair weather conditions, these devices will harvest energy constantly provided that the railcar is in motion.

EXPERIMENTAL SETUP AND PROCEDURES

Laboratory testing was carried out on the UTCRS dynamic bearing test rigs. These test rigs include a single bearing tester (SBT), pictured in Figure 2, and a four bearing tester (4BT), shown in Figure 3. These testers were designed to mimic the operating conditions of class K (6½"×9"), class F (6½"×12"), class G (7"×12"), and class E (6"×11") tapered roller bearings in rail service. For class K and F bearings, each bearing supports a load of 153 kN (34.4 kip) at full railcar load. To maintain fidelity, both testers are fitted with similar hydraulic cylinders capable of applying up to 150% of the full railcar load. In contrast, an empty railcar load is equivalent to 17% of the full load or 26 kN (5.85 kips). The testers are powered by 22 kW (30 hp) variable frequency motors that can simulate maximum train speeds of 137 km/h (85 mph).

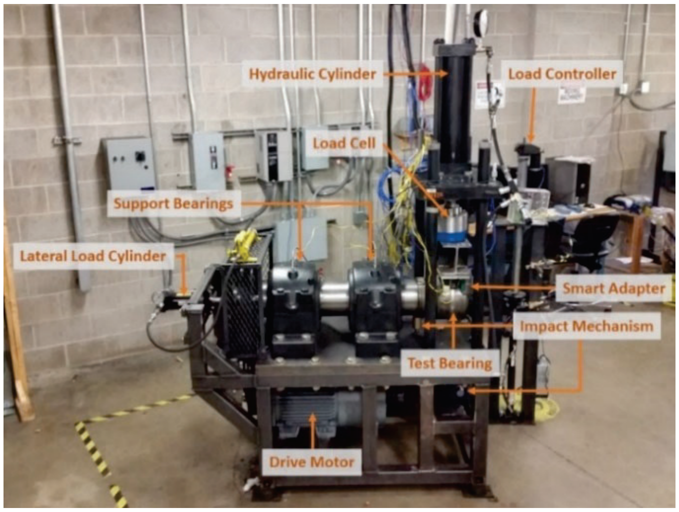

Figure 2: Single Bearing Tester (SBT)

Figure 3:Four Bearing Tester (4BT)

The testers are equipped with industrial-size fans that can supply a constant airflow to the axle/bearing assembly simulating the forced air convection experienced in rail service when the train is in motion. The fans generate an airstream with an average velocity of 6 m/s. A bearing adapter was modified to accommodate both the energy harvesting device and the wireless condition monitoring module intended to be powered (see Figure 4). To obtain temperature data during experiments, a combination of K-type bayonets and K-type thermocouples are strategically placed to monitor and record the bearing operating temperature as well as the bearing adapter temperature relative to the ambient conditions. The thermocouples are connected to a National Instruments (NI) PXIe-1062 data acquisition system (DAQ) which employs LabVIEW^{TM} to record the temperatures.

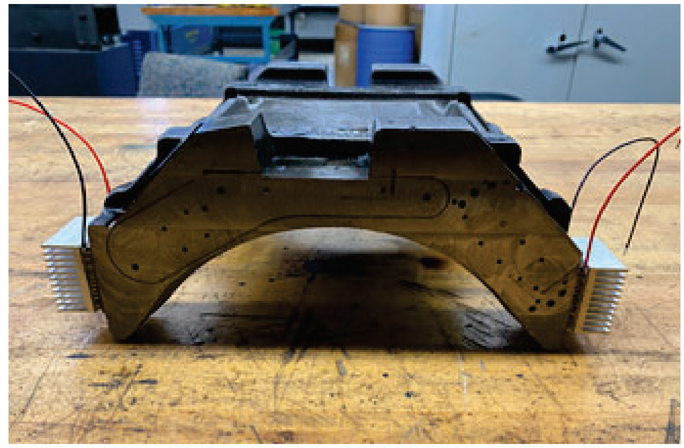

Figure 4: Bearing Adapter with mounted TEGs

To produce the required voltage, two TEGs were installed on both sides of the adapter, as seen in Figure 4, and connected in series to add their voltages. The schematic diagram of Figure 5 shows how the TEG modules are connected in series, and have their voltage collected and measured across the resistor with an NI USB6008 data acquisition card.

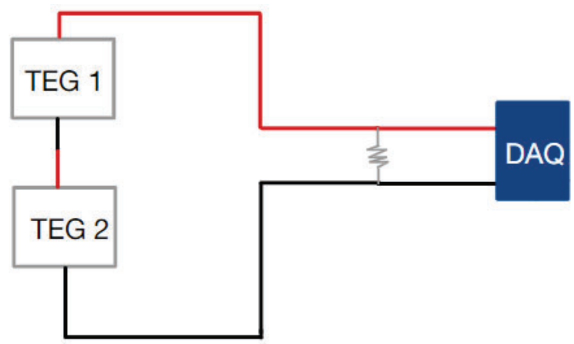

Figure 5: Schematic of TEG devices wired in series with DAQ

Using two TEGs ensures optimal operation regardless of wind direction as a harvesting system; using a single TEG would be less efficient when the train travels in the opposite direction of its installation location. Two different types of thermoelectric generators were used which included the TEG2-126LDT body scavenger (40×40 mm) and the TEG1-1263-4.3 (30×30 mm). Other than surface area, the main difference between both TEGs utilized in this study is that the TEG2-126LDT is designed to work at lower temperature gradients unlike the TEG1-1263-4.3 which is more efficient at higher temperature gradients. Both thermoelectric generators have semiconductors made of Bi_3Te_3 (Bismuth Telluride). They are mounted to the edges of the bearing adapter using a thermal adhesive with a thermal conductivity, k, of $0.9\,\frac{W}{m\cdot k}$ which fills the voids between the TEG and the adapter surface in order to maximize contact surface area and heat transfer. This mounting solution is only meant for laboratory testing. In field service, a more rugged method should be employed to affix the thermoelectric generators to the bearing adapter, providing optimal thermal performance as well as convenient replacement of the TEGs if the need arises.

Two commercially available circuit boards were used to step up the voltage obtained from the TEGs to a voltage sufficient to charge the rechargeable lithium batteries. The first circuit used is a buck-boost converter that uses an input voltage ranging from 0.9 to 5 V and boosts the voltage to 5 V. The converter module is rated to 600 milli-amps, but in this application, it will be operated at an estimated 7 to 8 mA output at the optimum power. The buck-boost converter is then connected to a TP4067 battery charging module which will regulate the voltage to a safe operating range while it recharges the lithium batteries. This battery management chip offers a charging cut-off voltage of 4.2 V to safeguard the battery from damage.

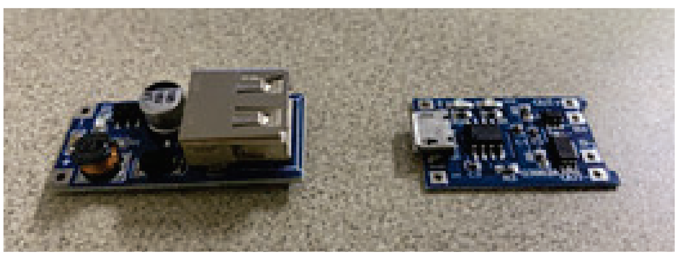

Figure 6: Buck-boost converter (left); battery management chip (right)

The battery management chip, pictured in Figure 6 (right), has output terminals for both the battery and the load applied to the chip, i.e., the wireless condition monitoring module in our current application. When the buck booster does not provide sufficient voltage to the battery management chip, the wireless module will be powered by the auxiliary 3.7 V lithium battery. When there is a sufficient temperature gradient for the TEG devices to provide the required voltage, the battery management chip will charge the battery while the battery continues to power the wireless health monitoring module. The batteries used are the 14500 rechargeable lithium-ion batteries that have a nominal voltage of 3.7 V. For this study, numerous laboratory experiments were performed to evaluate both the performance of the individual thermoelectric generators used and the overall energy harvesting system efficacy under several varying operating conditions. The testing results are discussed hereafter.

RESULTS AND DISCUSSION

In the following experimental results, the optimal power, P_{opt}, and optimal resistance, R_{opt}, values were calculated, respectively, using Eq. (1) and Eq (2) provided hereafter.

$$P_{opt} = \frac{V_{oc} \cdot I_{sc}}{4} \tag{1}$$

$$R_{opt} = \frac{V_{oc}}{I_{sc}} \tag{2}$$

Thermoelectric Generator Performance

The TEG device individual performance was assessed using a simple circuit that consisted of a resistor in series with the TEG acting as a voltage source. For this experiment, a hot plate was used as a heat source for the "hot" side of the TEG while the "cold" side utilized a heat sink and fan cooling solution. When the temperatures reached steady state, the difference between each side was roughly 15˚C. Once the voltage and current were determined, the resistor was replaced for a different value. The resistors used included 2, 3, 11, and 15 ohms (Ω). Figure 7 and Figure 8 show the linear trend behavior obtained from the different voltage and current values across the different resistors for both TEGs. These trends were used to obtain the open circuit voltage, V_{oc}, and the short circuit current, I_{sc}, values.

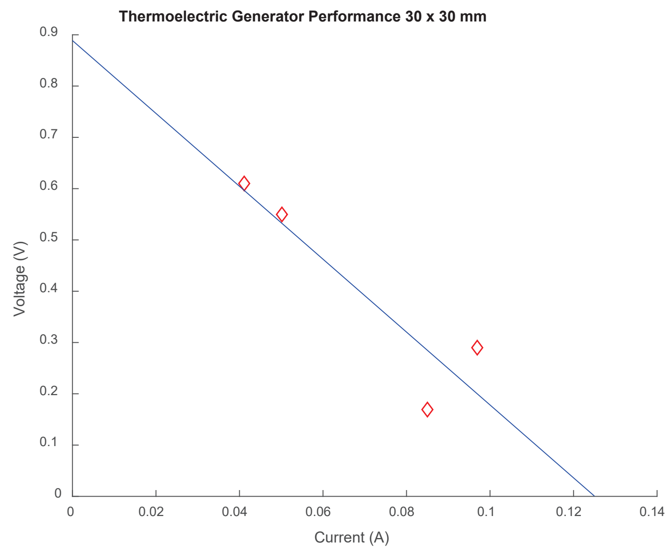

Figure 7: Performance of 30×30 mm TEG

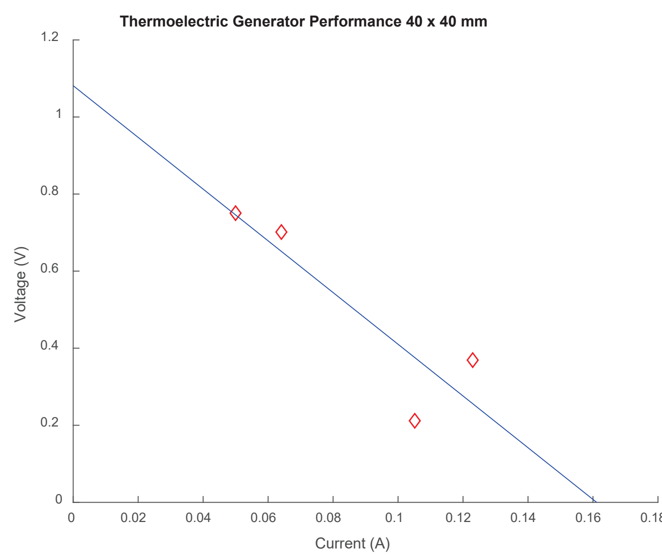

Figure 8: Performance of 40×40 mm TEG

From Figure 7 and Figure 8, the V_{oc} and I_{sc} values are determined to be 0.888 V and 0.125 A for the 30×30 mm TEG and 1.081 V and 0.161 A for the 40×40 mm TEG. Using Eq. (1), the optimal power for this set of resistors was calculated to be 27.8 mW for the 30×30 mm TEG and 43.5 mW for the 40×40 mm TEG. Equation (2) gives the optimal resistance needed for the TEG modules to achieve optimal power. The optimal resistance for the 30×30 mm and 40×40 mm TEGS was determined to be 7.1 and 6.7 Ω, respectively.

Experiment 228B

In this experiment, the performance of the harvesting device under different bearing applied loads was explored. The resulting data was used to determine the optimal load resistance value for optimized TEG device operation. This experiment was performed on the SBT at two different loads, 17% load simulating an empty railcar load and 100% load corresponding to a full railcar load. The motor was set at a constant 560 RPM which corresponds to a train traveling at a speed of 97 km/h (60 mph). This is a common speed for freight railcars traveling in rural areas. The resistor values used for this experiment included 20, 46.6, 100, 150, and 200 Ω. The data collected for this experiment included voltage and temperature data from the ambient surrounding the tester and the temperature of the bearing adapter. Since the overall efficacy of the energy harvesting device was being assessed, the individual temperatures of both sides of the TEGs were not used. Instead, the generated voltages were derived from the temperature difference between the adapter surface where the TEG is mounted and the ambient conditions. Figure 9 displays the voltages produced at 17% load (empty railcar) across the set of resistors listed earlier. Figure 10 shows the temperature difference between the ambient and the bearing adapter.

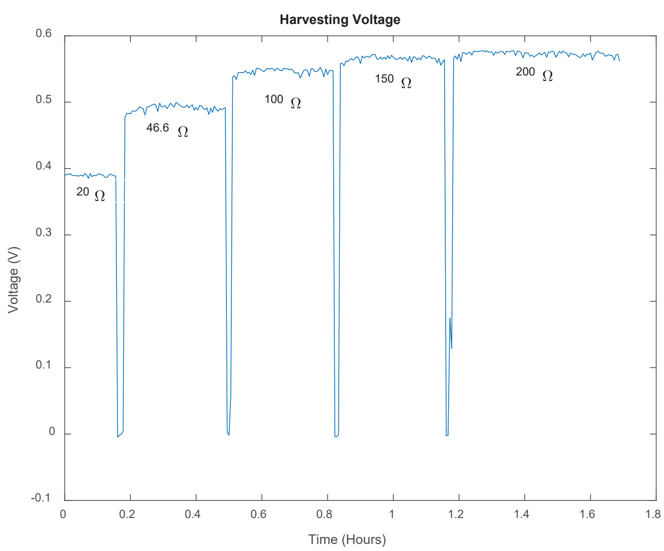

Figure 9: Voltages produced at 17% load (empty railcar) across 20, 46.6, 100, 150, and 200 Ω resistors

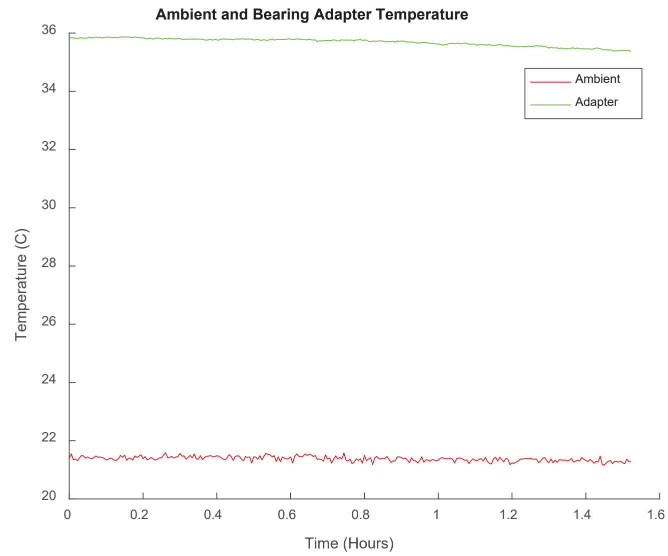

Figure 10: Temperature difference between the ambient and the bearing adapter temperatures at 17% load (empty railcar)

In Figure 10, it can be seen that the ambient temperature remained fairly constant throughout the experiment, while the adapter temperature dropped slightly (< 1˚C) towards the end of the experiment. The average temperature difference between the ambient and the bearing adapter was about 14.4˚C where the mean temperatures of the bearing adapter and the ambient were 35.8˚C and 21.4˚C, respectively. From Figure 9, the voltage readings increased as the resistor value increased with diminishing returns as larger resistances were used. The sudden voltage drops seen in Figure 9 represent the instances at which the resistors were being swapped in the circuit. Table 1 lists the average voltage, current, and power obtained from each resistance used in this experiment.

Table 1: Average values for voltage, current, and power at 17% load (empty railcar)

40×40 mm TEG			
Resistance [Ω]	Average Voltage [V]	Average Current [A]	Average Power [mW]
20	0.389	0.019	7.6
46.6	0.484	0.010	5.0
100	0.542	0.005	2.9
150	0.561	0.004	2.1
200	0.566	0.003	1.6

From the data summarized in Table 1, it can be seen that as the resistance increased, both the current and the power decreased. The data shows that the optimum load resistance is below 20 Ω; however, the voltage at this point is too low for our boost converter; and even at higher load resistances the voltage has not increased to a usable level.

Since the results obtained at an empty railcar load (17%) did not produce favorable conditions, the load was increased to 100% corresponding to a full railcar load. Figure 11 and Figure 12 provide the results of testing at steady state conditions.

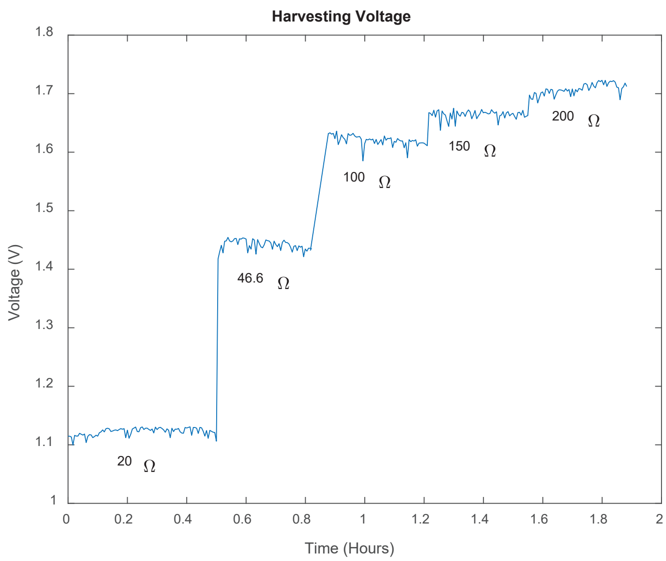

Figure 11: Voltages produced at 100% load (full railcar) across 20, 46.6, 100, 150, and 200 Ω resistors

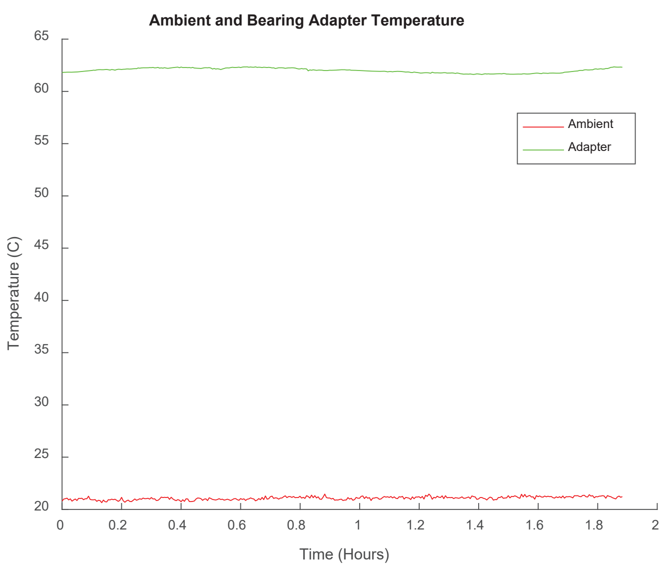

Figure 12: Temperature difference between the ambient and the bearing adapter temperatures at 100% load (full railcar)

Figure 12 demonstrates the temperature difference between the ambient and bearing adapter while the tester was subjected to 100% load. While the laboratories' mean ambient temperature stayed consistent at 21˚C, the mean bearing adapter temperature increased to 62˚C. At these temperatures, the temperature difference increased the optimum to 41˚C or 2.8 times greater than previous temperatures at 17% load. Following previous trends, Figure 11 shows the increase in voltage as the resistance increased.

Table 2: Average values for voltage, current, and power at 100% load (full railcar).

40×40 mm TEG			
Resistance [Ω]	Average Voltage [V]	Average Current [A]	Average Power [mW]
20	1.120	0.056	62.7
46.6	1.449	0.031	45.1
100	1.621	0.016	26.3
150	1.664	0.011	18.5
200	1.708	0.009	14.6

Table 2 was generated using the data in Figure 11. This data shows that the optimum load resistance is below 20 Ω; however, at this resistance, the voltage is sufficient to properly operate the boost converter. In addition, the highest power harvesting was recorded at the same resistance with a value of 63 mW. Using the data from both Table 1 and Table 2, it is clear that in order to determine the optimal range of the harvesting devices, new load resistance values would have to be tested in order to demonstrate operation at the optimal harvesting point.

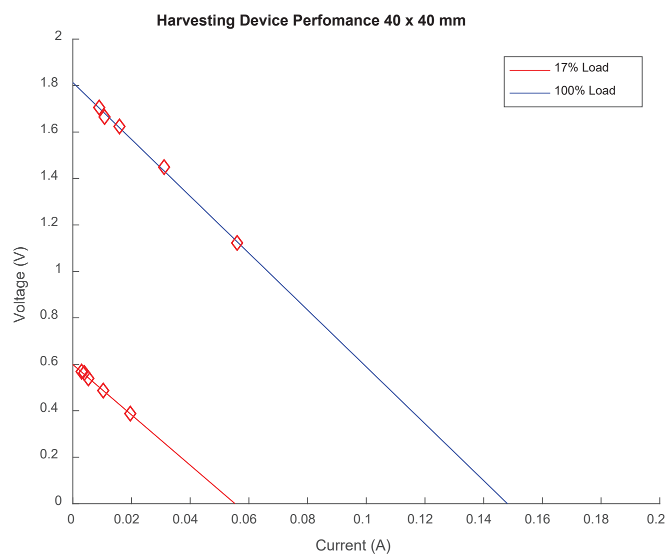

Figure 13: Harvesting device performance at 17% and 100% load across 20, 46.6, 100, 150, and 200 Ω resistors

By plotting the values from both Table 1 and Table 2, the V_{oc} and I_{sc} values were determined again using a linear trend. Figure 13 shows the V_{oc} and I_{sc} values for 17% load to be 0.599 V and 0.055 A, respectively, while at 100% load, the values were 1.813 V and 0.142 A, respectively. Using Eqs. (1) and (2), the optimal power and resistance at both loads (17% and 100%) were again calculated. For 17% load, the optimal power and resistance was 8 mW and 10.9 Ω, respectively, while at 100% load, the values were 64 mW and 12.8 Ω, respectively. With these new theoretical values, a new set of resistors were tested to determine the best optimal resistance at which the harvesting device would operate. Hence, the new set of resistors chosen were 2, 5, 7, 10, and 15 Ω. The experiments were then repeated at both 17% and 100% loads. Figure 14 through Figure 18 along with Table 3 and Table 4 present the results for the new set of resistors.

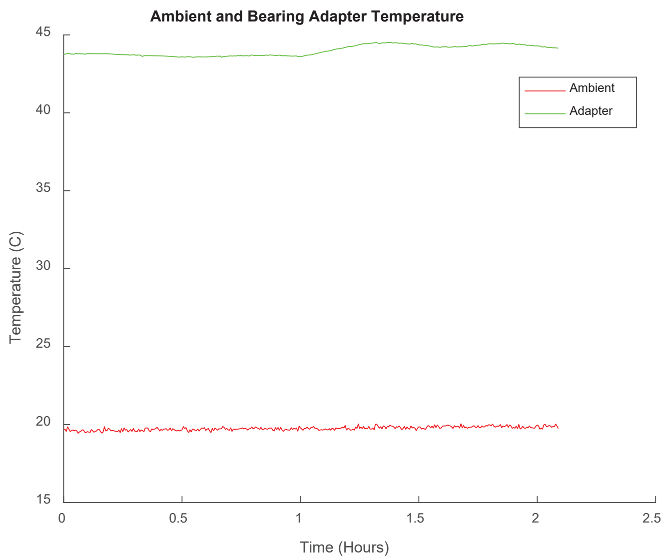

Figure 14: Temperature difference between the ambient and the bearing adapter temperatures at 17% load (empty railcar)

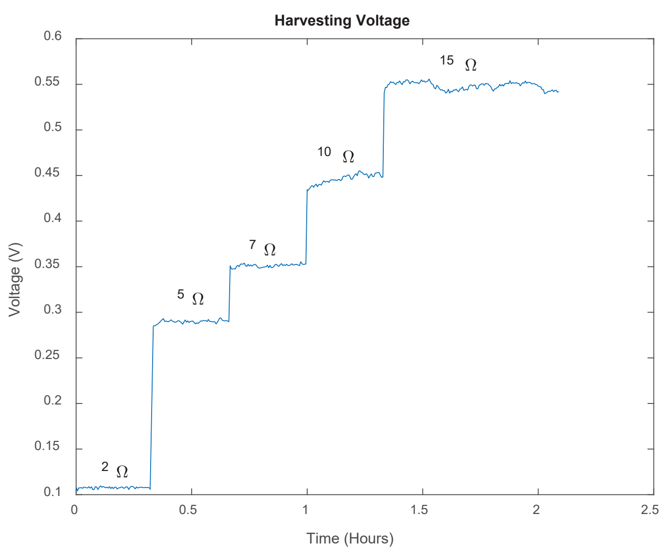

Figure 15: Voltages produced at 17% load (empty railcar) across 2, 5, 7, 10, and 15 Ω resistors

In Figure 14, the mean ambient temperature was 20˚C while the mean adapter temperature was 44˚C, creating a temperature difference of 24˚C. Unlike the resistances in Table 1, the tested resistances in Table 3 are mostly below the optimum resistance value. From the data, it appears the optimum resistance is between 10 and 15 Ω as expected, with a maximum available power of about 20 mW. However, at 17% load, the voltage at the maximum power is not sufficient to start the boost converter.

Table 3: Average values for voltage, current, and power at 17% load (empty railcar)

40×40 mm TEG			
Resistance [Ω]	Average Voltage [V]	Average Current [A]	Average Power [mW]
2	0.107	0.054	5.8
5	0.289	0.058	16.8
7	0.351	0.050	17.6
10	0.447	0.045	20.0
15	0.548	0.037	20.0

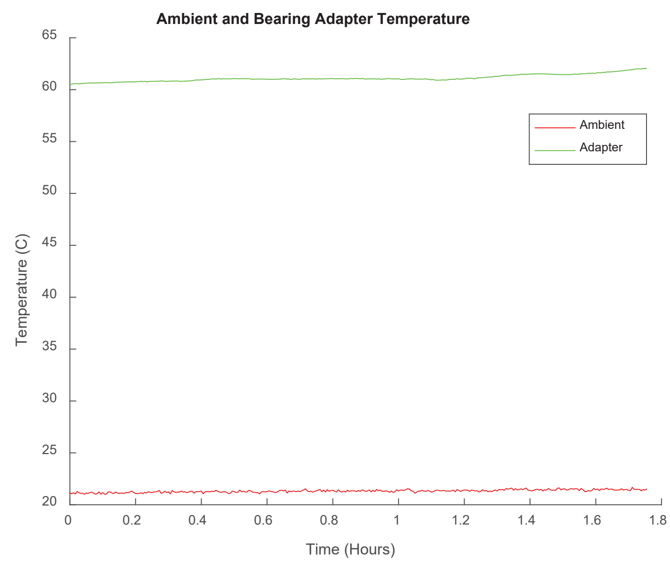

Figure 16: Temperature difference between the ambient and the bearing adapter temperatures at 100% load (full railcar)

Table 4: Average values for voltage, current, and power at 100% load (full railcar)

40×40 mm TEG			
Resistance [Ω]	Average Voltage [V]	Average Current [A]	Average Power [mW]
2	0.188	0.188	17.7
5	0.513	0.513	52.7
7	0.627	0.627	56.1
10	0.775	0.775	60.0
15	0.959	0.064	61.4
20	1.120	0.056	62.7
46.6	1.449	0.031	45.1
100	1.621	0.016	26.3
150	1.664	0.011	18.5
200	1.708	0.009	14.6

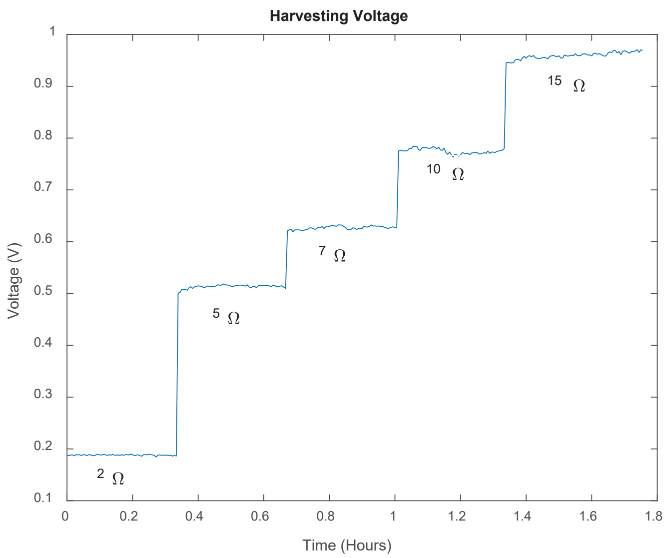

Figure 17: Voltages produced at 100% load (full railcar) across 2, 5, 7, 10, and 15 Ω resistors

The load was then increased again to 100% producing Figure 16 and Figure 17 along with Table 4 which includes the results from the previous series so that the optimum point can be clearly seen. At 100% load, a temperature difference of 40˚C was determined from the recorded mean ambient temperature of 21˚C and mean adapter temperature of 61˚C. This temperature difference was closer to the previous test (100% load) using the initial set of resistors maintaining consistency across results. The optimum load resistance is between 15 and 20 Ω with a maximum available power of about 62 mW. The voltage at the optimum is around 1.1 V which is sufficient to start the boost converter.

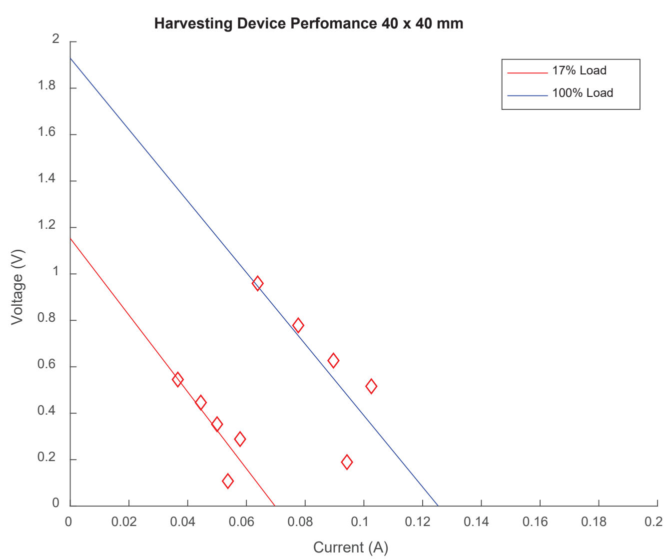

Figure 18: Harvesting device performance at 17% and 100% load across 2, 5, 7, 10, and 15 Ω resistors

Figure 18 was plotted by creating a linear fit using the data gathered from Table 3 and Table 4. In this plot, at 17% load, the V_{oc} and I_{sc} values were found to be 1.153 V and 0.070 A, respectively, while at 100% load the values were 1.929 V and 0.125 A respectively. Using Eqs. (1) and (2) yields an optimal power and resistance of 20 mW and 16.5 Ω, respectively, for 17% load and 60 mW and 15.4 Ω respectively for 100% load. With this data, it is concluded that the optimal resistance for this harvesting device setup is 15 Ω, producing the highest mean power of 61 mW.

Experiment 227C

To determine the performance of a harvesting device using TEG1-1263-4.3 harvesters, they were installed on the 4BT tester. The 4BT continuously runs at full speed 796 RPM (i.e., 137 km/h or 85 mph) and full load. This experiment should be representative of a best-case scenario as they are ideal conditions for high heat generation in the bearings. Figure 19 and Figure 20 depict the temperature difference and the harvesting voltage obtained during this experiment.

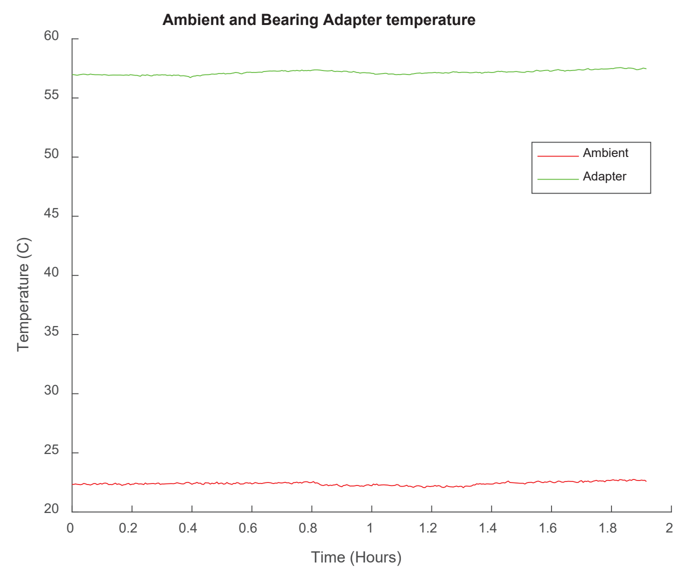

Figure 19: Temperature difference between the ambient and the bearing adapter temperatures at 100% load (full railcar)

In Figure 19, the mean temperature of the bearing adapter was at 57˚C while the ambient mean temperature was 22˚C. These temperatures produced an average temperature difference of 35˚C. Examining Figure 20, it can be observed that the voltage increased as the resistance increased, displaying diminishing returns at higher resistor values. From Table 5, at the highest resistance of 200 Ω, a mean voltage of 0.573 V was produced. In contrast, at the lowest resistance of 20 Ω, a voltage of 0.375 V was produced. At 20 Ω, the average power recorded was highest with a value of 7 mW while at 200 Ω, the lowest mean power was recorded at 1.6 mW. With these values, the TEG1-1263-4.3 at 100% load performs like the TEG2-126LDT at 17% load.

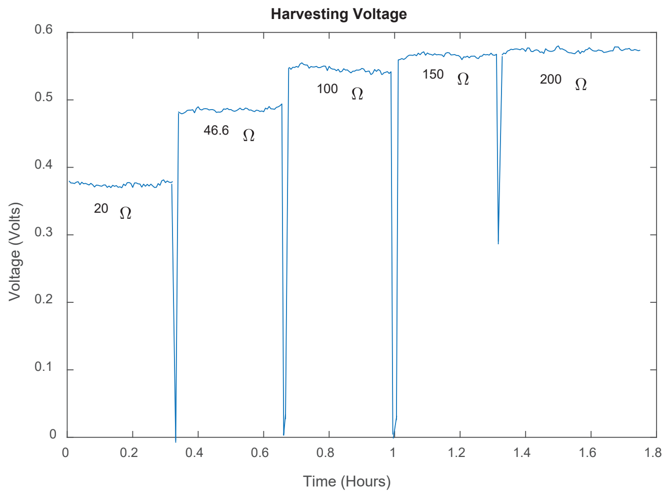

Figure 20: Voltages produced at 17% load (empty railcar) across 20, 46.6, 100, 150, and 200 Ω resistors

Table 5: Average values for voltage, current, and power at 100% load (full railcar)

30×30 mm TEG			
Resistance [Ω]	Average Voltage [V]	Average Current [A]	Average Power [mW]
20	0.375	0.019	7.0
46.6	0.485	0.010	5.1
100	0.545	0.005	3.0
150	0.566	0.004	2.1
200	0.573	0.003	1.6

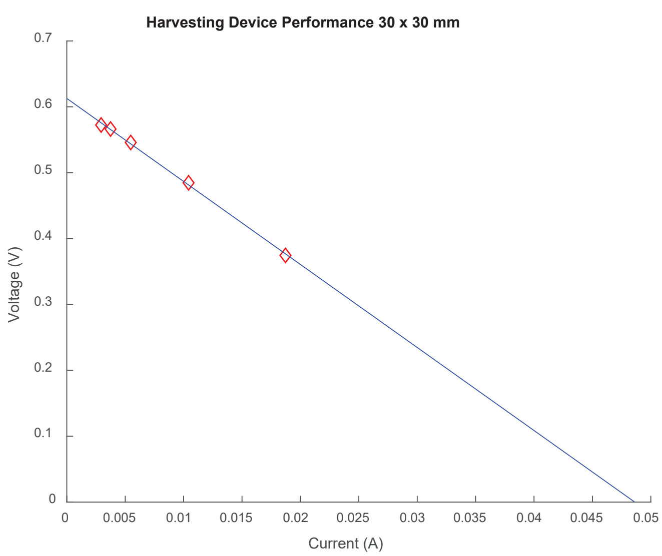

Figure 21: Harvesting device performance at 100% load across 20, 46.6, 100, 150, and 200 Ω resistors

From Figure 21, the V_{oc} and I_{sc} are 0.613 V and 0.046 A respectively. Using Eqs. (1) and (2), the optimal power and resistance can be computed yielding 7 mW and 13.3 Ω, respectively. With these results, it can be concluded that even in ideal conditions, the voltage produced by the TEG1-1263-4.3 harvesters is not sufficient to operate the boost converter in our application. To provide a sufficient voltage using these TEGs, either a higher temperature gradient will have to be introduced, or more TEGs will have to be connected in series.

CONCLUSION

By using thermoelectric generators, the wasted heat produced by the tapered roller bearings can be converted to electrical energy for powering bearing health monitoring devices. This harvesting solution stands out due to its solid-state design, minimizing its maintenance when compared to other methods. If successful, the harvesting device will be able to produce sufficient electrical energy to power the wireless condition monitoring module provided that the railcar remains in motion. From the information gathered in these experiments, it has been proven with confidence that, in certain operating conditions, there is a sufficient temperature difference to recharge the 14500 battery, thus, extending its usable life.

From the data gathered in the experiments, the TEG1-1263-4.3 (30×30 mm) module does not perform to the desired specifications with good reason. Unlike the TEG2-126LDT (40×40 mm), it is not designed to work at relatively low temperature deltas. Instead, its smaller form factor made it an attractive option as it can be placed in more locations throughout the bearing adapter to harvest more energy if needed. Even at full speed and load, the harvesting device fitted with the TEG1-1263-4.3 was not able to meet the required performance. Instead, these devices serve as a good option to add if more energy is needed than what can be delivered using only two TEG2-126LDT units. When subjected to the right operating conditions, the TEG2-126LDT harvesting device can generate 60 mW of power at 15.4 Ω. At this rate, it will be able to fully charge the 14500 battery (4070 mWh) within 67 operating hours. Future experimentation will monitor the current produced using the buck booster and battery management system. With this data, the power after losses can be obtained in order to determine if the rate of power generated can be consistently greater than the rate of power consumed. This information can be used to quantify the total usable lifespan of the rechargeable battery.

REFERENCES

[1] D.M. Rowe, G. Min, "*Evaluation of thermoelectric modules for power generation*", Journal of Power Sources 73 (1998) 193-198.

[2] S.B. Riffat, X. Ma, "*Thermoelectrics: a review of present and potential applications*", Applied Thermal Engineering, 23 (2003): 913-935.